

EXPERIMENTS ON THE BEAM-BEAM EFFECT

IN  $e^+ e^-$  STORAGE RINGS\*

H. Wiedemann  
Stanford Linear Accelerator Center  
Stanford University, Stanford, California 94305

(Invited talk presented at the Symposium on Nonlinear Dynamics and the Beam-Beam Interaction, Brookhaven National Laboratory, Upton, New York, March 19-21, 1979.)

---

\* Work supported by the Department of Energy under contract number EY-76-C-03-0515.

## I. Introduction

The maximum luminosity in a positron electron storage ring is fundamentally limited by the beam-beam effect. This is the perturbing effect of the electromagnetic field of one beam on the trajectory of every single particle of the other beam. The electromagnetic field of a charged particle beam is highly nonlinear. At a large distance from the beam center the field falls off like the inverse of the distance. Right in the center of the beam where we have a more or less uniform density distribution over a limited region the field rises linear with the distance from the center. So the field rises from the center of the beam, saturates at some distance and going further out falls off again as  $1/r$ . The amplitude of the field depends on the charge density as well as the aspect ratio of the beam. If the electromagnetic field of one beam gets too large, particles of the other beam get lost which leads to a reduced beam lifetime. This effect has been observed in all electron-positron or electron-electron storage rings built so far and is considered the fundamental limit of the performance of electron-positron storage rings.

Over the years many measurements have been performed at various laboratories to find the maximum permissible perturbation and the parametric dependences of that perturbation. In this paper new measurements performed at SPEAR are presented and compared with measurements from ACO,<sup>1</sup> ADONE,<sup>2</sup> and VEEP-2M.<sup>3</sup> Results from other storage rings have been ignored because they either show lower permissible perturbations or because of insufficient published data.

## II. Phenomenology of the Beam-Beam Effect

During the process of filling a storage ring with electrons or positrons both beams are customarily separated at the collision points by the use of electrostatic fields. When a current in both beams sufficiently large to exhibit a beam-beam effect but not too large to be destructive is stored the electric fields are turned off within a few microseconds. In all experiments the intensity of both beams is equal. With both beams colliding we make the following general observation by looking at the beam cross-section as transmitted via the synchrotron light:

- both beams are blown up vertically
- there is no significant horizontal blow up ( $\leq 10\%$ )
- one of the beams is blown up much more than the other one.

Figure 1(a) shows the two beam cross sections while the beams are still separated. In Fig. 1(b) the blown up cross-sections of colliding beams are shown. The beam cross-sections as shown in Fig. 1 are those at two different points in the ring both not at the interaction point. Therefore, the horizontal width of both beams is slightly different even when separated (Fig. 1(a)). In Fig. 2 photometric measurements of the horizontal (x) and vertical (y) beam cross-section for separated and colliding beams are shown for two different beam currents. Within the accuracy of the measurement there is no beam blow up for two colliding beams of 1 mA each, however, for a beam current of 4 mA we measure an increase of the beam height of about a factor two. The resolution of the system is about 0.25 mm.

In SPEAR the large blow up of one of the beams can be avoided by properly phasing the RF-cavities positioned symmetrically about the

interaction points,<sup>4</sup> thereby maximizing the luminosity. Because this cavity phasing can make either beam to be blown up with respect to the other we call this effect the flip-flop effect. Figure 1(c) shows the beam cross sections in the balanced state. It is believed that the flip-flop phenomenon is caused by a small horizontal separation of the centers of the beams at the interaction. This also has been observed and investigated at ACO.<sup>5</sup> The variation of the beam cross section with beam current can be derived from the luminosity measurements for different colliding currents. We expect the luminosity  $L$  to scale like

$$L = \frac{I^2}{e^2 \cdot f_0 \cdot A} \quad (1)$$

with  $I = I^+ = I^-$  the beam current,  $f_0$  the revolution frequency and  $A$  the beam cross-section at the interaction point assumed to be the same for both beams. Figure 3 shows that up to a threshold current the luminosity scales like  $I^2$ . Above this threshold the luminosity is lower than expected. From Eq. (1) we expect that this is the regime where the beams get blown up. Since there is no horizontal beam blow up the ratio of the expected to actual luminosity is just equal to the vertical blow up of the core of the beams. As we increase the current beyond the threshold the luminosity increases<sup>6</sup> like  $L \sim I^{1.3}$  and the beams get more and more blown up. The current limit and with it the maximum luminosity is reached when after bringing both beams into collision one of them exhibits a short lifetime. In practice, the limit is reached at somewhat lower currents because before any reduction in lifetime is observed the amount of background for the experimental detectors increases significantly.

We conclude from these observations that the beam-beam effect blows up the vertical beam size as a function of the intensity of the colliding beams. The limit is reached when the extreme tails of the density distribution reach the aperture limit which first causes increased background and then a reduction in beam lifetime. From the luminosity measurements or the beam size measurements using the synchrotron light we only can derive the dimensions of the core of the beam (up to  $2\sigma$  for a Gaussian beam). Background and beam lifetime, however, are determined by the particles in the far out tails of the distribution. Since it is not obvious from luminosity measurements how the large amplitude particles are affected by the beam-beam effect the density distribution in the tails has to be measured separately. This we have done in SPEAR for single as well as colliding beams.

The density distribution in the tails is measured with the use of beam scrapers by observing the reduction of beam lifetime as a function of the position of the scrapers. In electron-positron storage rings the density distribution is expected to be Gaussian. For such a distribution the beam lifetime is given by<sup>7</sup>

$$\tau = \frac{1}{2} \tau_{\beta} \frac{e^{\zeta}}{\zeta} \quad (2)$$

where  $\tau_{\beta}$  is the transverse damping time and  $\zeta = \frac{s^2}{2\sigma_{\beta}^2}$  with  $\sigma_{\beta}$  the transverse standard deviation of the beam size and  $s$  the position of the scrapers.

We measure the beam lifetime for a scraper position  $s_M$ , correct that lifetime for the residual gas lifetime and then calculate the ratio  $s/\sigma_{\beta}$  from Eq. (2) to give the same lifetime. For a truly Gaussian beam

the quantity  $s/\sigma_\beta$  should be a linear function of  $s_M$ . In Figs. 4 and 5 the results of these measurements together with the beam size measurement in the center of the beam are plotted for separated and colliding beams.

It is seen clearly that in the horizontal plane the density distribution is Gaussian for a single beam up to about  $5.5 \sigma_{\beta x}$ . At larger amplitudes there is a long tail which appears in all measurements. These tails may be caused by nonlinearities. In the vertical plane the density distribution for a single beam is not quite Gaussian which might be due to nonlinear coupling between the horizontal and vertical plane.

For colliding beams we observe little blow up of the horizontal beam size in the center but significantly more in the tails. Much more dramatic, however, is the blow up of the vertical tails which is of the order of a factor 5 compared to a factor of 2 in the center of the beam. It is this large vertical blow up that requires a vertical acceptance of the storage ring that is larger than expected from beam size measurements of the core.

### III. Parametric Dependencies of the Beam-Beam Effect

In order to understand more about the beam-beam effect measurements of the limit as a function of many parameters have to be performed. To characterize the beam-beam effect it has become customary to measure or calculate the linear tune shift for small amplitude particles due to the space charge field of the other beam. As mentioned before, the electromagnetic field in the center of the beam increases linearly with the distance from the center. This is the characteristic field of a quadrupole which causes a shift in the betatron frequency, the tune of the storage ring, when both beams are brought into collision. Since all

higher-order components of the space charge field are strictly proportional to the linear component the linear tune shift is a characteristic quantity for the whole nonlinear field. The linear tune shift is given by

$$\xi_{x,y} = \frac{r_e}{2\pi e f_0 B \gamma} \frac{I \beta_{x,y}}{\sigma_{x,y} (\sigma_x + \sigma_y)} \quad (3)$$

where  $r_e$  the classical electron radius,  $e$  the electric charge unit,  $f_0$  the revolution frequency,  $B$  the number of bunches per beam,  $\gamma$  the beam energy in  $mc^2$ ,  $I$  the beam current,  $\beta_{x,y}$  the horizontal or vertical betatron function at the interaction point and  $\sigma_x, \sigma_y$  the beam sizes at the interaction point. Since generally  $\xi_x < \xi_y$ , we use only  $\xi_y = \xi$  in the rest of this paper. The Eq. (3) assumes a Gaussian distribution which is always sufficiently the case in the core of the beam. To calculate the linear tune shift from Eq. (3) requires the accurate knowledge of the beam sizes at the interaction point. This is best done by measuring the luminosity:

$$L = \frac{1}{4\pi e^2 f_0} \frac{I^2}{B \sigma_x \sigma_y} \quad (4)$$

If we combine Eqs. (3) and (4) and eliminate  $\sigma_x \cdot \sigma_y$  we get

$$\xi = 2r_e e \frac{L/I}{\gamma} \frac{\beta_y}{1 + \frac{\sigma_y}{\sigma_x}} \quad (5)$$

Here all quantities on the right hand side can be measured except for  $\sigma_x/\sigma_y$ . This ratio, however, is rather well known in cases where the beams are fully coupled like in ADONE or ACO or is very small like in SPEAR and, therefore, can be ignored. In a simple model used so far

for the design of storage rings it is assumed that there is a maximum value for  $\xi$  (usually 0.06) independent of other parameters. With this assumption ( $\xi_{\max} = \text{constant}$ ) we would expect the luminosity to scale like

$$L \sim \xi_{\max}^2 \gamma^2 \frac{B \epsilon_x}{\beta_y^{3/2}} \sim \xi_{\max}^2 \gamma^4 \frac{B}{\beta_y^{3/2}} \quad (6)$$

with  $\epsilon_x$  the horizontal beam emittance ( $\epsilon_x \sim \gamma^2$ ). In the rest of this paragraph we will discuss the validity of this model.

In SPEAR and other storage rings measurements have been performed to determine the parametric dependence of the maximum tune shift which we will discuss in the remainder of this section:

$\xi_{\max} = f(\beta_y)$ : According to Eq. (6) the luminosity is expected to vary inversely proportional to  $\beta_y^{3/2}$  with all other relevant parameters staying constant. In SPEAR the maximum luminosity was measured as a function of  $\beta_y$  and is shown in Fig. 6 together with the tune shift. It is evident that below a certain value of  $\beta_y$  - here about 10 cm - there is no gain in luminosity any more. In fact, the luminosity even drops to lower values. A possible explanation could be the fact that the bunch length  $\sigma_z \approx 2$  to 3 cm becomes comparable with the value of the beta function. Especially particles in the tails (5 to 6  $\sigma_z$ ) of the longitudinal density distribution will collide with the core of the other beam at some distance from the interaction point and therefore at larger values of  $\beta_y$ . Further measurements on that point, however, are required.

$\xi_{\max} = f(v_x, v_y, v_s)$ : A strong dependence of the maximum achievable linear tune shift with the tune of the storage ring has been predicted.<sup>8,9</sup>

Measurements at ADONE<sup>2</sup> and SPEAR<sup>10</sup> confirm this prediction which generally

states that in electron-positron storage rings the beam-beam limit increases as the vertical tune approaches an integer from higher values. This can clearly be seen in Fig. 7 from Ref. 10.

During these measurements the horizontal tune was kept constant at  $\nu_x = 5.20$  for  $5.189 > \nu_y > 5.117$ . For the case  $\nu_y = 5.10$  the horizontal tune had to be lowered to  $\nu_x = 5.15$  in order to avoid the resonance line  $2\nu_y - \nu_x = 5$  which we would have had to cross for  $\nu_x = 5.20$  on the way from the injection configuration to the collision configuration.

It is interesting to note that this resonance  $2\nu_y - \nu_x = 5$  is a "forbidden" resonance in the 2-fold symmetry SPEAR. Indeed, for a single beam this resonance cannot be detected. In the two beam operation, however, this line is strong enough to destroy one of the beams, an indication that due to the strong beam-beam nonlinearities "forbidden" ordinary betatron resonances appear very strong in higher-order terms. With the change in SPEAR of the RF-frequency from 50 MHz to 350 MHz in 1974 the strong dependence of the beam-beam limit with  $\nu_y$  vanished almost completely. The only cause for that we can think of is that with the higher RF-frequency the synchrotron frequency increased from values  $\nu_s < .01$  to values of  $\nu_s \approx .03$ . The synchrotron frequency causes synchrobetatron oscillations which appear as satellites of the integer tune. For small values of  $\nu_s$  all relevant satellites are very close to the integer tune while for  $\nu_s = 0.03$  they spread over the whole tune diagram. It is the appearance of these narrow spaced resonances which we believe makes the tune dependence of the beam-beam limit vanish in SPEAR. Obviously more measurements are in order to verify this.

$\xi_{\max} = f(\delta x, \delta y)$ : As discussed in Section II the luminosity and thereby

the beam-beam limit depend very sensitively on the separation  $\delta x$  and  $\delta y$  of the beams at the interaction point. Every possible effort should be made to minimize beam center separation to avoid the before-mentioned flip-flop phenomenon.

$\xi_{\max} = f(E, \epsilon_{ytot}, n_{IP})$ : In this paragraph we want to investigate the dependence of the beam-beam limit on the energy ( $E$ ), the storage ring acceptance or total beam emittance ( $\epsilon_{ytot}$ ) (including the tails) and the number of interaction points ( $n_{IP}$ ). From Eq. (6) we expect with otherwise constant parameters the luminosity to scale like the fourth power of energy  $L \sim E^4$ . In Fig. 8 the measured energy dependence of the maximum achieved luminosities are shown for ACO,<sup>1</sup> ADONE,<sup>2</sup> and VEEP-2M,<sup>3</sup> together with measurements from SPEAR. The solid lines are fits with  $L \sim E^6$ . It is obvious that all the measurements show a stronger energy dependence than the simple model of Eq. (6) would predict. It should be noted that physicists of the different storage ring groups fit their measurement differently (ACO:  $L \sim E^{5.4}$ , ADONE:  $L \sim E^7$ , and VEEP-2M:  $L \sim E^4$ ). As can be seen, however, from Fig. 8, a  $L \sim E^6$  fit works very well for all machines. In the case of VEEP-2M the published<sup>3</sup> luminosity vs. energy curve has a distinct step at about 450 MeV. It is believed by the author of this paper that at this point the tune and thereby the beam size has been changed to maximize the luminosity at lower energies. This was mentioned in Ref. 3 but it was not made obvious at what energy and by how much the tune was changed.

For the rest of this paper we assume there is a universal beam-beam effect in all four storage rings that makes the maximum achievable luminosity scale like

$$L \sim E^6 \quad (7)$$

It should be mentioned, however, that above a certain energy indicated by an arrow  $\uparrow$  in Fig. 8 the luminosity all of a sudden levels off or even drops again. For VEEP-2M this is so because of technical reasons which limit the current that can be stored. In SPEAR this "transition" energy coincides with the maximum injection energy. Operation at higher energies requires the beams to be brought from the injection energy up to higher energies. This prevents the operators in SPEAR from making little improvements over a longer period of time when all the ring magnets are in a steady state. In cases where energy ramping is required the end configuration never is exactly the same since the different magnets track differently. However, the difference between achieved and expected luminosity is large and one can suspect that some other effect as yet unexplored may come into play. This notation is also nourished by the ADONE data. The injection energy in ADONE is 350 MeV and therefore the energy always has to be ramped yet the luminosity levels off only above 1 GeV. For the rest of this paper we consider only that energy regime in which the luminosity scales like  $E^6$ . From the luminosity measurements of Fig. 8 we can calculate the linear tune shift if the beam current is known. In Fig. 9, the tune shift parameter  $\xi$  as a function of energy is plotted for ADONE<sup>2</sup> and SPEAR. All measurements from ADONE involve 6 interaction points while SPEAR only has 2 interaction points. For ACO and VEEP-2M no data for the beam currents were available to calculate the  $\xi$ -parameter. From Fig. 9, we conclude that the maximum linear tune shift is a linear function of energy and not as commonly assumed, a constant:

$$\xi_{\max} \sim E \quad (8)$$

In Section II it was described how the vertical beam blow up increases with increasing beam current until the aperture limit is reached. We have investigated this in more detail in SPEAR. With the help of a scraper the total vertical beam size was measured as a function of the beam current. In Fig. 10, the result of such a measurement is shown. We plot the tune shift parameter versus the square root of the total beam emittance for reasons that will become apparent in the next section. The result of the measurement looks very surprising. For a small beam-beam effect the beam size is large then decreases with increasing beam-beam effect and finally increases again. Since this variation of the beam size has been observed for different configurations it must be assumed to be real. The large tails, and this is all we measure here, at low currents are consistent with the tails observed in single beams (see Fig. 5) and could be caused by the nonlinear magnetic field of the sextupoles. Addition of the beam-beam nonlinearity reduces at first the amplitude of the tails for reasons as yet not investigated. Only for  $\xi$ -parameters larger than .02 we observe the expected beam blow up, which is consistent with the observation in Fig. 3.

The maximum achievable tune shift parameter usually is assumed to be independent of the number of interaction points in a storage ring. This assumption is in disagreement with the observations from ACO<sup>1</sup> and ADONE<sup>2</sup> the only storage rings where the number of interaction points can be changed still preserving a machine symmetry of at least two. In both storage rings it was observed that the maximum value of  $\xi$  is reduced as

the number of interaction points is increased. The data are consistent with a scaling of

$$\xi_{\max} \sim \frac{1}{\sqrt{n_{\text{IP}}}} \quad (9)$$

which we will assume to be correct in the following section.

#### IV. Try of an Empirical Scaling Law for the Linear Tune Shift

##### Parameter $\xi_{\max}$

From experiments on the beam-beam effect we found the parameter  $\xi_{\max}$  to vary like the energy of the beams. We also observe while the beam-beam effect blows up the vertical beam size this blow up reaches a steady state amplitude depending on the beam current. This behavior rules out an instability or a strong resonance to be the cause for the beam-beam limit. Whatever the mechanism to blow up the beam, it seems in electron-positron storage rings to be successfully counteracted by the damping due to synchrotron radiation. In order to test the parametric dependence of the maximum tune shift parameter  $\xi_{\max}$  we try the following model:

The total vertical betatron emittance  $\epsilon_{y\text{tot}}$  changes with time due to damping like<sup>7</sup>

$$\frac{d}{dt} \sqrt{\epsilon_{y\text{tot}}} = - \frac{\sqrt{\epsilon_{y\text{tot}}}}{2\tau_y} \quad (10)$$

with  $\tau_y$  the damping time. This damping is counteracted in the case of colliding beams by the beam-beam effect. We assume the blow up to be caused by a diffusion-like process as suggested, for example, by H. G.

Hereward<sup>11</sup> and J. R. LeDuff.<sup>12</sup> Without using any theoretical derivation we assume the vertical beam size blow up to be proportional to the strength of the nonlinear field and the betatron amplitude at the interaction point or, in other words, the blow up is proportional to  $\xi$ . If one or more resonances are the driving source for the diffusion process not only the strength of the nonlinear field but also the amplitude of the particle plays an important role. It is well known that nonlinear resonances affect mostly large amplitude particles which are just the ones that limit the beam lifetime if they get scraped at the walls of the vacuum chamber. We try, therefore, the blow up rate to scale like  $\frac{d}{dt} \sqrt{\epsilon_{ytot}} \sim \epsilon_x$  using  $\epsilon_x$  rather than  $\epsilon_y$  because the observation shows that the large amplitude particles are almost fully coupled in the horizontal and vertical phase plane and  $\epsilon_x$  is a well known quantity in electron-positron storage rings. Since the beam-beam effect only changes the slope of the particle's trajectory but not the amplitude we assume the square root of the total emittance  $\sqrt{\epsilon_{ytot}}$  to change linearly with time rather than  $\epsilon_{ytot}$ . We further assume that the rate of growth of the vertical amplitude depends on the number of collisions per unit time. For a diffusion-like process the amplitude growth rate should scale like the square root of the number of collisions per second. With this model we get a growth rate which scales like:

$$\frac{d}{dt} \sqrt{\epsilon_{ytot}} \sim \xi_{max} \epsilon_x \sqrt{\frac{n_{IP}}{C}} \quad (11)$$

where  $C$  is the circumference of the storage ring.

Both damping [Eq. (10)] and excitation [Eq. (11)] lead to an equilibrium with:

$$\xi_{\max} = \mu \frac{\sqrt{\epsilon_{ytot}}}{\epsilon_x \tau_y} \sqrt{\frac{C}{n_{IP}}} \quad (12)$$

where  $\mu$  is a constant and  $\epsilon_{ytot}$  the total vertical beam emittance.

From a dimensional point of view Eq. (11) is not very satisfactory, but since we do not know the exact mechanism of the beam-beam blow up we bury all dimensions in the proportionality constant  $\mu$  and use Eq. (12) only as a guide for experiments and as a possible empirical scaling law.

In Eq. (12), we discover first the correct energy dependence. Since  $\epsilon_x \sim E^2$  and  $\tau_y \sim E^{-3}$  we find  $\xi_{\max} \sim E$  in agreement with measurements at ADONE and SPEAR (Fig. 9). With the maximum beam-beam parameter  $\xi_{\max} \sim E$  we arrive at a luminosity scaling like  $L \sim E^6$ . This is in agreement with all the observations as shown in Fig. 8. The dependence of  $\xi_{\max}$  on the square root of the number of interaction points is in agreement with observations in ADONE and ACO and supports therefore, strongly a diffusion process.

Fitting the measurements of Fig. 8 we get

$$\begin{aligned} \xi_{ADONE} &= -0.033 + 0.099 E(\text{GeV}) \\ \xi_{SPEAR} &= -0.035 + 0.044 E(\text{GeV}) \end{aligned} \quad (13)$$

and with the parameters of Table I:

$$\begin{aligned} \xi_{ADONE} &= -0.033 + 1.6 \times 10^{-8} \frac{\sqrt{\epsilon_{ytot}}}{\epsilon_x \tau_y} \sqrt{\frac{C}{n_{IP}}} \\ \xi_{SPEAR} &= -0.035 + 1.33 \times 10^{-8} \frac{\sqrt{\epsilon_{ytot}}}{\epsilon_x \tau_y} \sqrt{\frac{C}{n_{IP}}} \end{aligned} \quad (14)$$

Table I

	$\epsilon_{ytot}$ (rad m)	$\epsilon_x/E^2$ (rad m GeV <sup>-2</sup> )	$\tau_y/E^3$ (sec GeV <sup>-3</sup> )	C (m)	$n_{IP}$
ADONE	$45 \times 10^{-6}$	$11.7 \times 10^{-8}$	.038	100	6
SPEAR	$12 \times 10^{-6}$	$5.0 \times 10^{-8}$	.226	234	2

In spite of the very different values of the parameters involved for both machines the proportionality factors are close enough to be considered equal.

As opposed to Eq. (12), however, there appears a constant offset of -0.035 which we have to explain. Estimating the rate of vertical beam blow up we completely neglected the quantum fluctuations due to synchrotron radiation which gives an emittance growth rate of<sup>7</sup>

$$\frac{d\epsilon_x}{dt} = \frac{1}{2} \tau_x Q_x \left( \epsilon_x = \frac{\sigma_x^2}{\beta_x} \right) \quad (15)$$

where  $\tau_x = \tau_y$  is the betatron damping time and  $Q_x$  a quantity describing the quantized photon emission. The vertical beam emittance growth rate due to quantum fluctuations then is

$$\frac{d}{dt} \sqrt{\epsilon_{yQ}} = \frac{\tau_x Q_x}{4\sqrt{\epsilon_{yQ}}} \frac{K^2}{1+K^2} m^2 \quad (16)$$

where K is the coupling constant and  $m^2$  an amplitude factor necessary to account for the emittance of the tails. If we now add both growth rates from Eqs. (11) and (16) and solve for  $\xi_{max}$  we get

$$\xi_{\max} = \mu \frac{\sqrt{\epsilon_{ytot}} - \sqrt{\epsilon_{yQ}}}{\epsilon_x \tau_x} \sqrt{\frac{C}{n_{IP}}} . \quad (17)$$

Equation (17) exhibits the negative constant we were looking for since  $\epsilon_{yQ} \sim E^2$  and, therefore  $\sqrt{\epsilon_{yQ}} / (\epsilon_x \tau_x) \sim E^0$ . If we use the constant offset from Eq. (13) and solve for  $\epsilon_{yQ}$  in the case of SPEAR we get  $\epsilon_{yQ} = 1.9 \times 10^{-6}$  mm mrad. The  $\xi$  parameter and the associated total vertical beam emittance has been measured in SPEAR and is shown in Fig. 10. If we fit the last five points closest to  $\xi_{\max}$  we get

$$\xi_{\max} = -0.031 + 1.6 \times 10^{-8} \frac{\sqrt{\epsilon_{ytot}}}{\epsilon_x \tau_y} \sqrt{\frac{C}{n_{IP}}} \quad (18)$$

which is consistent within the errors of the measurements with Eq. (14).

The total vertical emittance of  $\epsilon_{ytot} = 1.9 \times 10^{-6}$  mm mrad at 2 GeV also is consistent with the density distribution measurement of Fig. 5 where we found at 1.55 GeV an emittance of  $\epsilon_{ytot} \approx 1.5 \times 10^{-6}$  mm mrad which gives 2.0 mm mrad at 2 GeV.

## V. Conclusion

The maximum achieved beam-beam parameter  $\xi$  has been measured in SPEAR and compared with other storage rings. At lower energies we found a consistent behavior of the beam-beam effect leading to a maximum luminosity to scale like  $L \sim E^6$  and a maximum beam-beam parameter scaling like  $\xi_{\max} \sim E$ . This is in contradiction to the generally assumed constant value of  $\xi_{\max}$  for the design of new storage rings. An empirical scaling law has been described which is consistent with the measurements available. The author is aware of the lack of detailed theoretical

background for this model but it helped to perform specific measurements which might be useful to finally understand the beam-beam effect in electron-positron storage rings.

In general, we conclude that the damping time and the vertical acceptance of the storage ring is of prime importance to reach large luminosities.

#### ACKNOWLEDGEMENTS

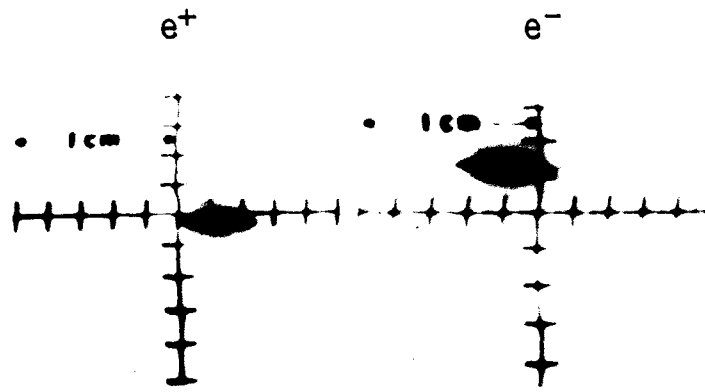
The author wishes to sincerely thank Tom Taylor and the SPEAR Operations Group for their continuous help and support in performing the measurements. This is especially true for the measurements of the maximum achieved luminosities at various energies which were taken in a large part from the operations logbooks as achieved while running SPEAR for high energy physics.

REFERENCES

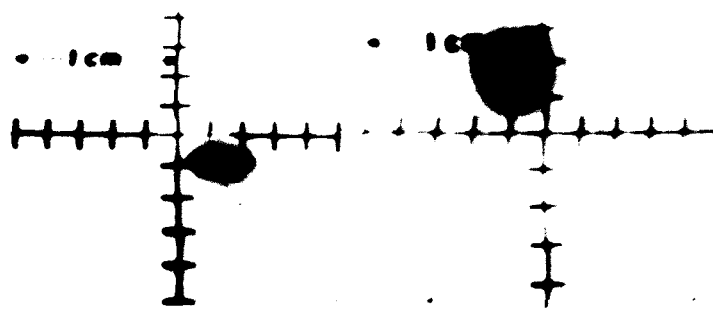
1. R. Belbeoch et al., Rapport Tech. 3-73 (1973).
2. Private communication from S. Tazzari. F. Amman et al., Proc. of the VIII International Conference on High Energy Accelerators, Geneva, 1971 (p. 132).
3. I. B. Vasserman et al., Proc. of the All-Union Conference on Charged Particle Accelerators, Dubna, USSR, 1978.
4. J. M. Paterson and M. Donald, 1979 Particle Accelerator Conference, San Francisco, March 12-14, 1979. An Investigation of the Flip-Flop Beam-Beam Effect in SPEAR.
5. R. Belbeoch et al., Internal Report NI/38-77, ORSAY 1977.
6. M. Cornacchia, PEP Note 275, Stanford, November 1978.
7. M. Sands, in Physics with Intersecting Storage Rings, ed. by B. Touschek, Academic Press, New York, 1971.
8. M. Bassetti, Proc. of the V International Conference on High Energy Accelerators, Frascati, 1965 (p. 708).
9. B. Richter, Proc. of the International Symposium on Electron and Positron Storage Rings, Saclay, 1966 (p. I-1-1).
10. SPEAR-Group, IEEE Trans. Nucl. Sci., Vol. NS-20, No. 3, 1973 (p. 838).
11. H. G. Hereward, CERN ISR-DI 72-26 (1972).
12. Y. R. LeDuff, ORSAY Rap. Tech. 6-72 (1972) and PEP Note 65 (1973).

FIGURE CAPTIONS

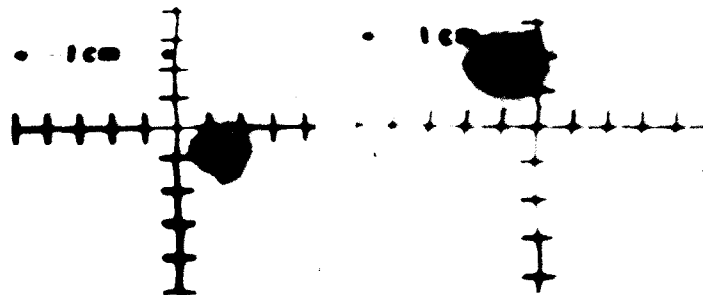
- Fig. 1. Beam cross-sections for separated and colliding beams.
- Fig. 2. Charge density distribution.
- Fig. 3. Luminosity vs. Beam Current.
- Fig. 4. Horizontal particle density distribution.
- Fig. 5. Vertical particle density distribution.
- Fig. 6. Luminosity and tune shift parameter  $\xi$  vs. the vertical betatron function.
- Fig. 7. Luminosity vs. beam current and vertical tune.
- Fig. 8. Maximum luminosity vs. energy.
- Fig. 9. Maximum tune shift vs. energy.
- Fig. 10. Tune shift parameter vs. total vertical beam emittance.



(a) Separated Beams



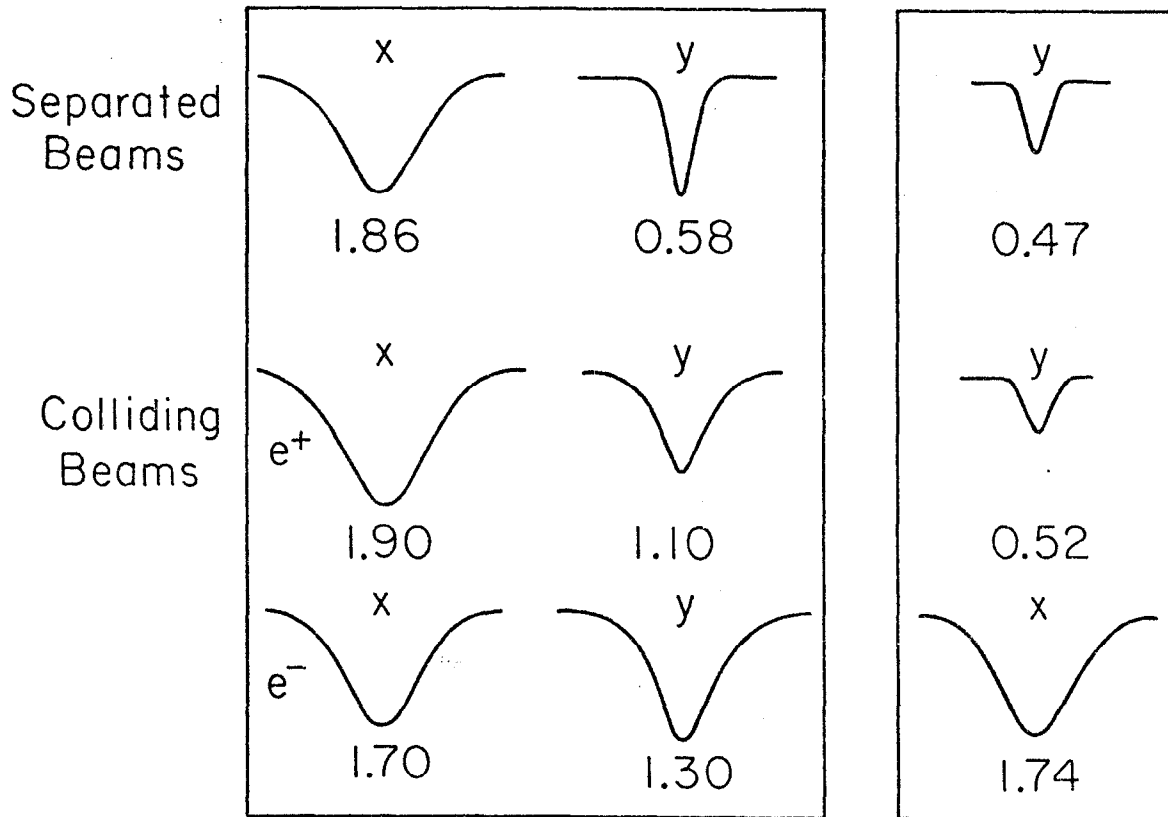
(b) Colliding Beams With Flip Flop Effect



(c) Colliding Beams Flip Flop Balanced

Fig. 1

BEAM SIZES FWHM (mm)



$4 \times 4 \text{ mA}^2$

$1 \times 1 \text{ mA}^2$

$E = 1.55 \text{ GeV}$        $\beta_y^* = 10 \text{ cm}$

Fig. 2

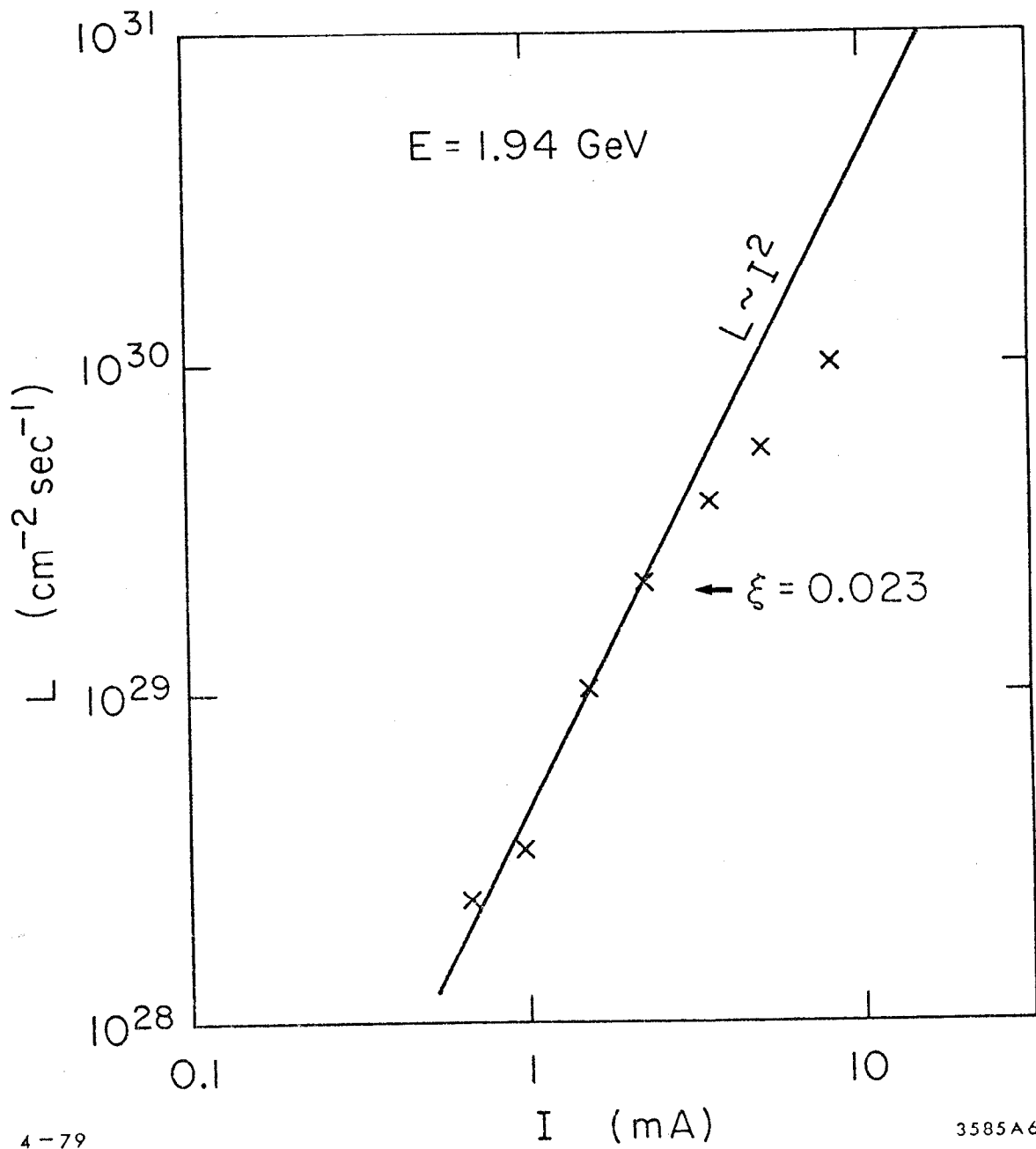


Fig. 3

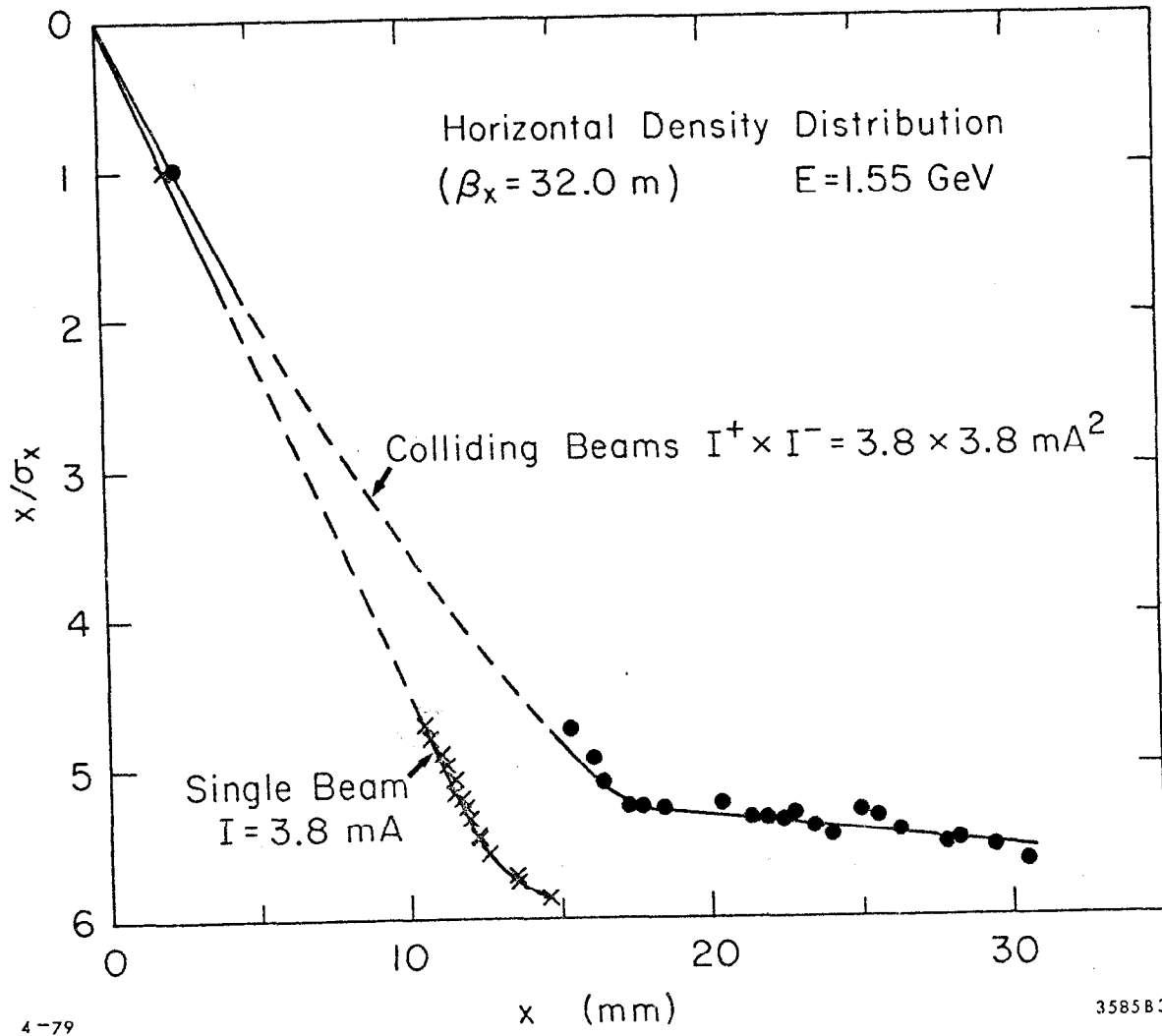


Fig. 4

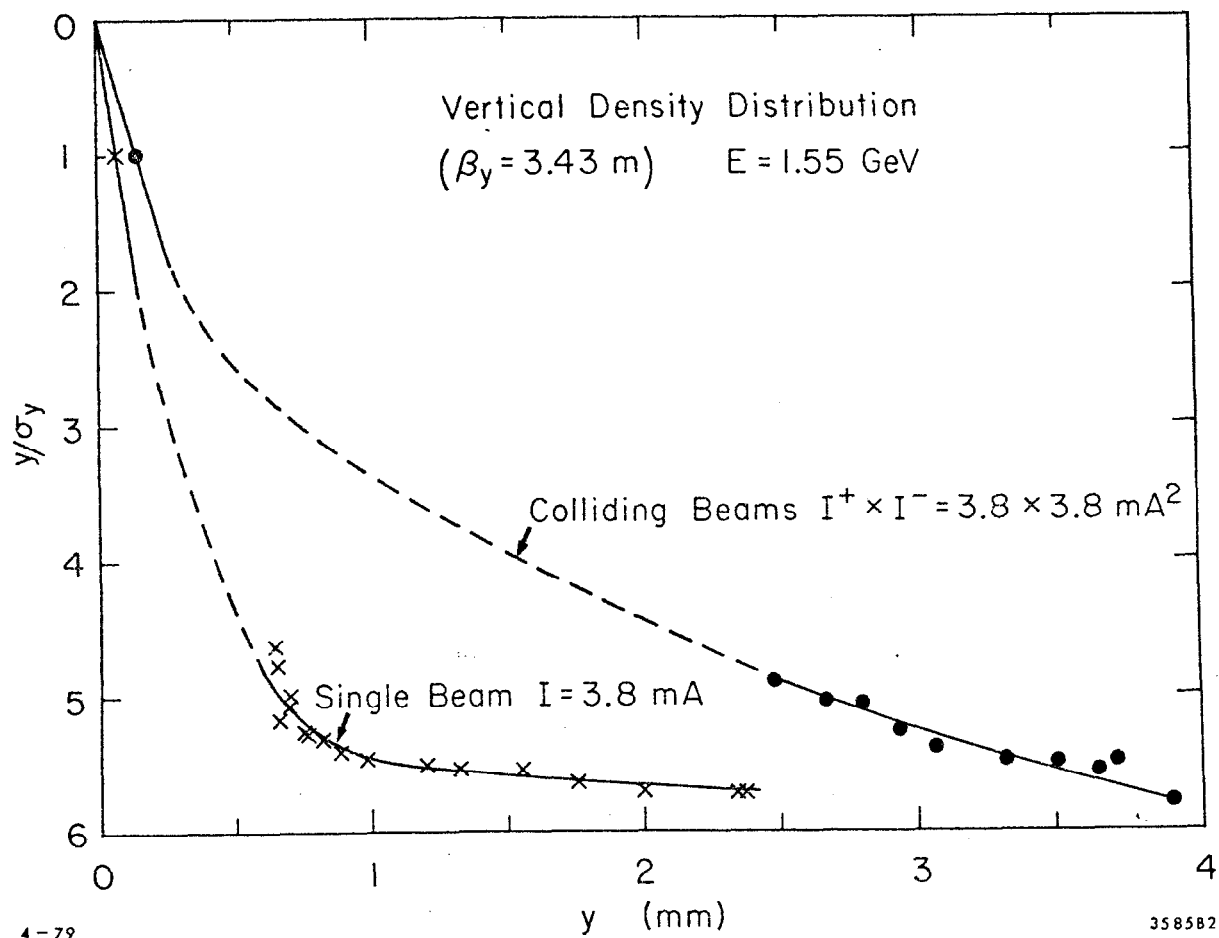
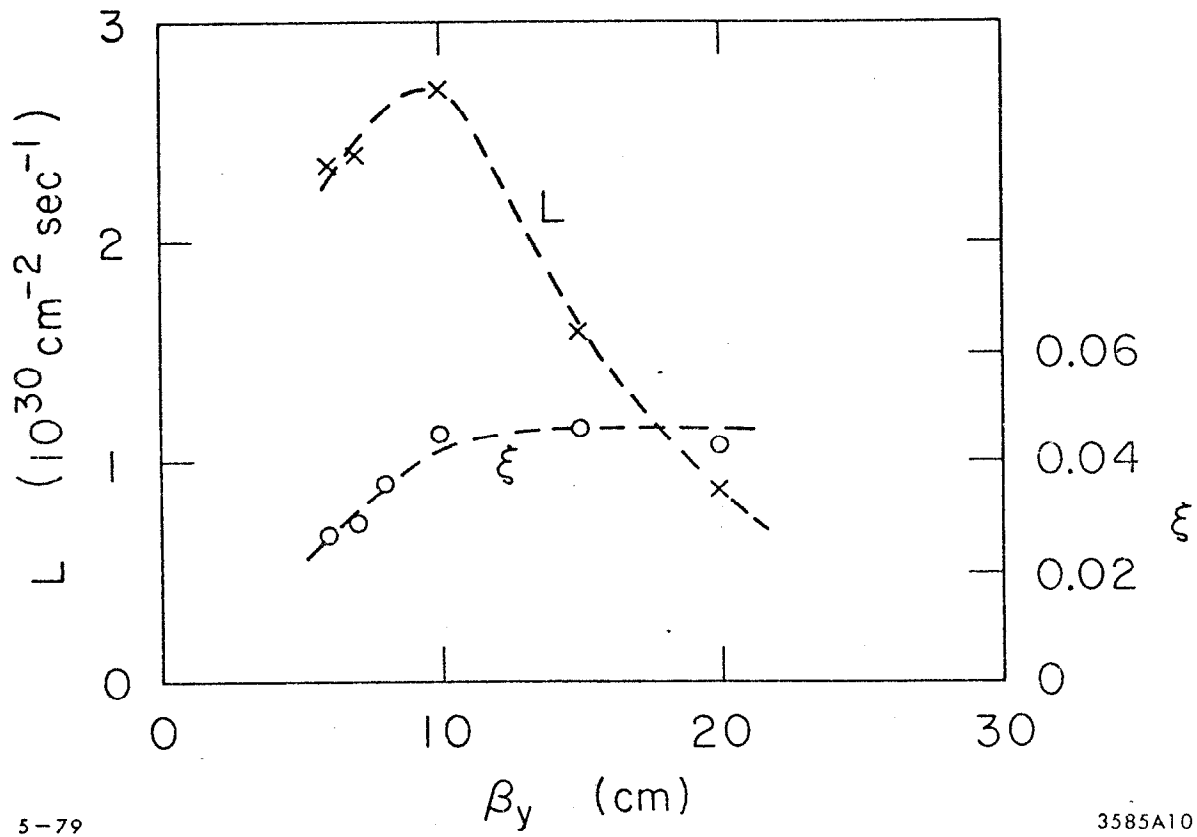


Fig. 5



5-79

3585A10

Fig. 6

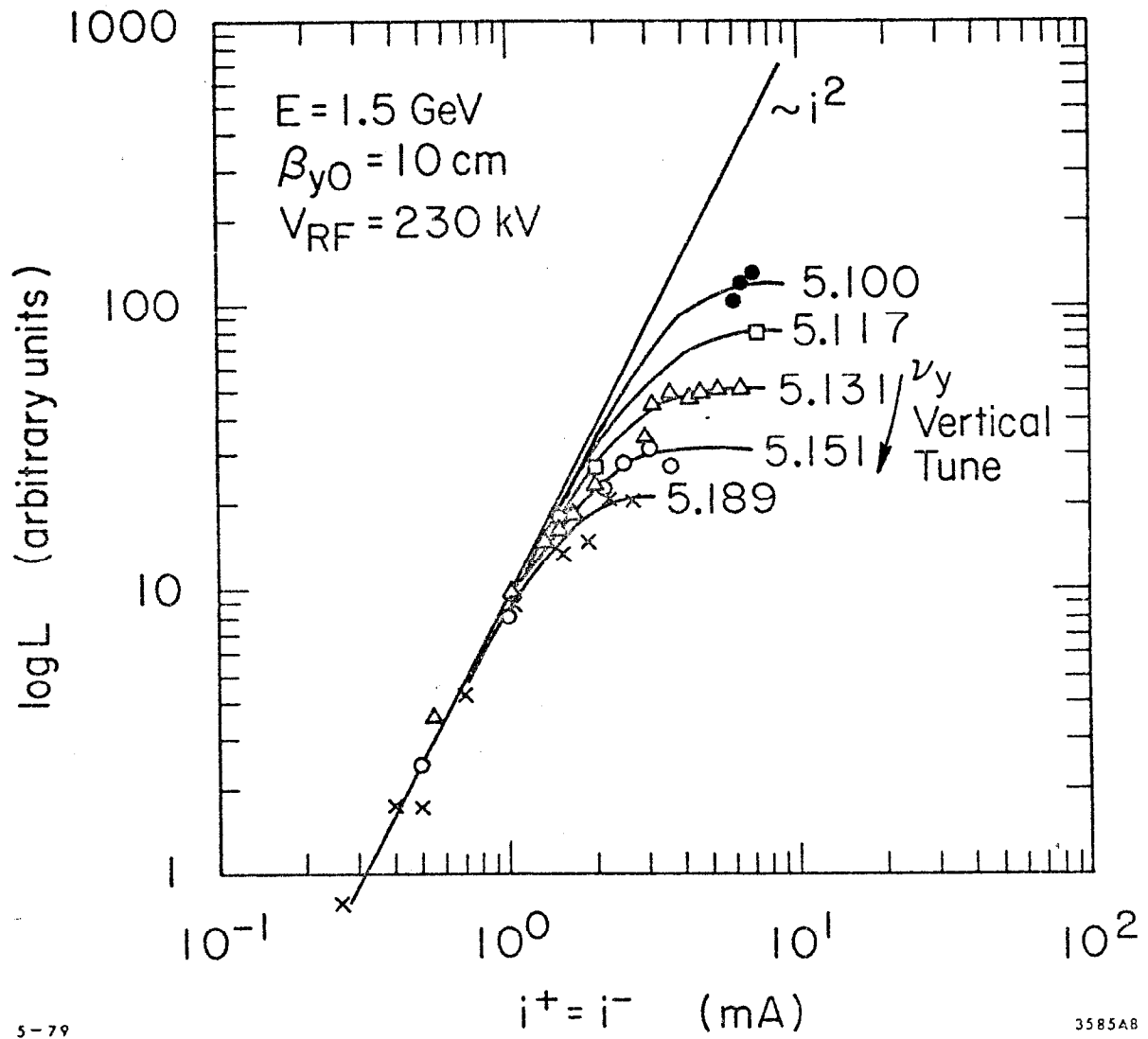


Fig. 7

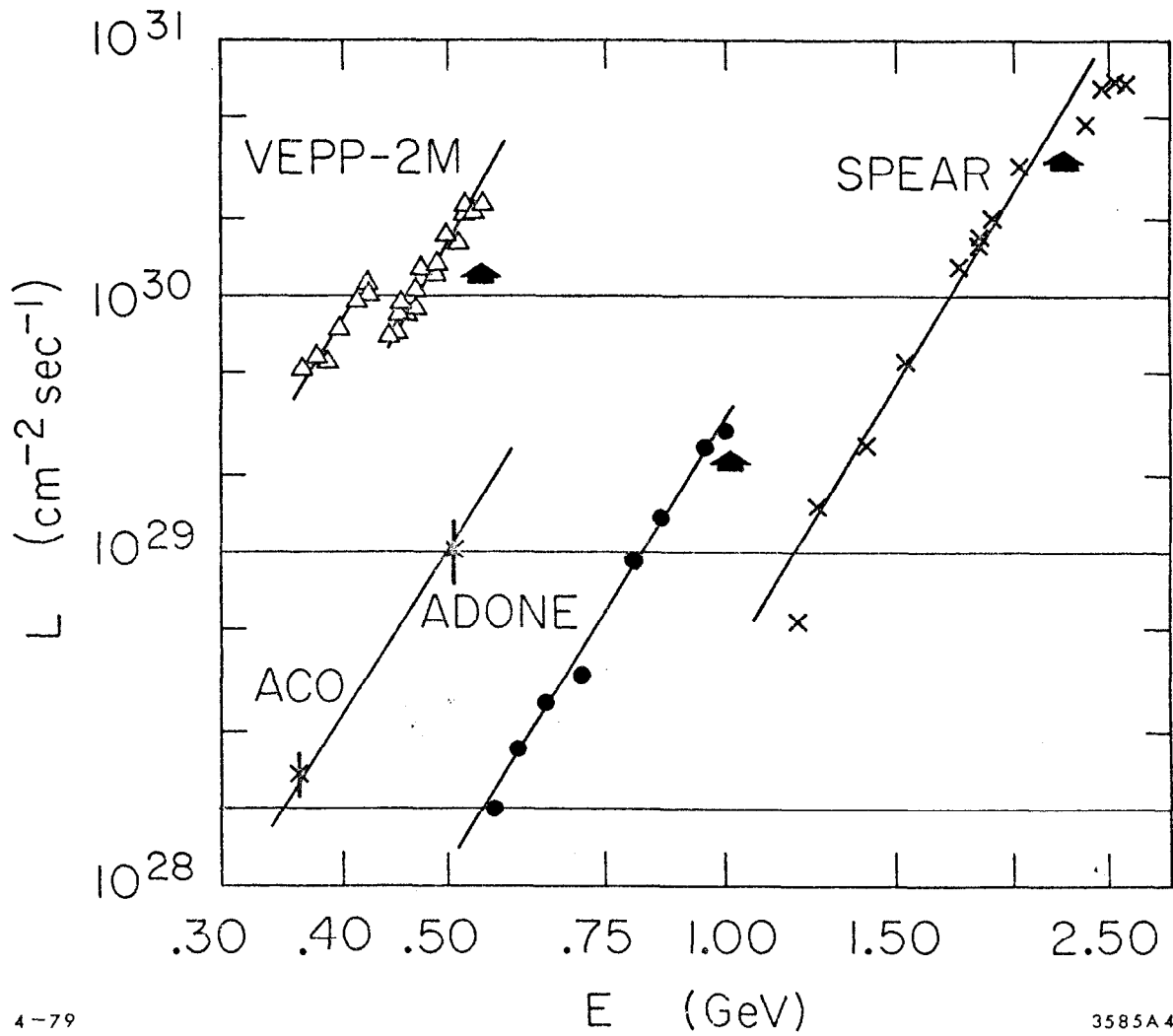


Fig. 8

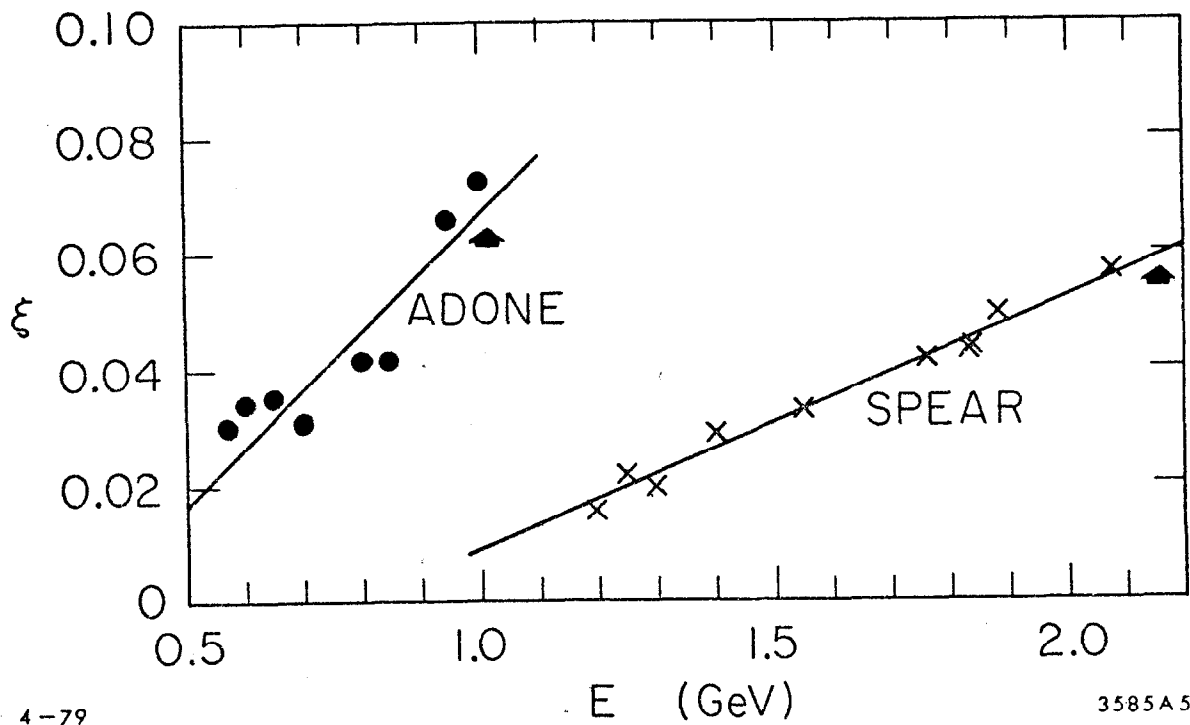
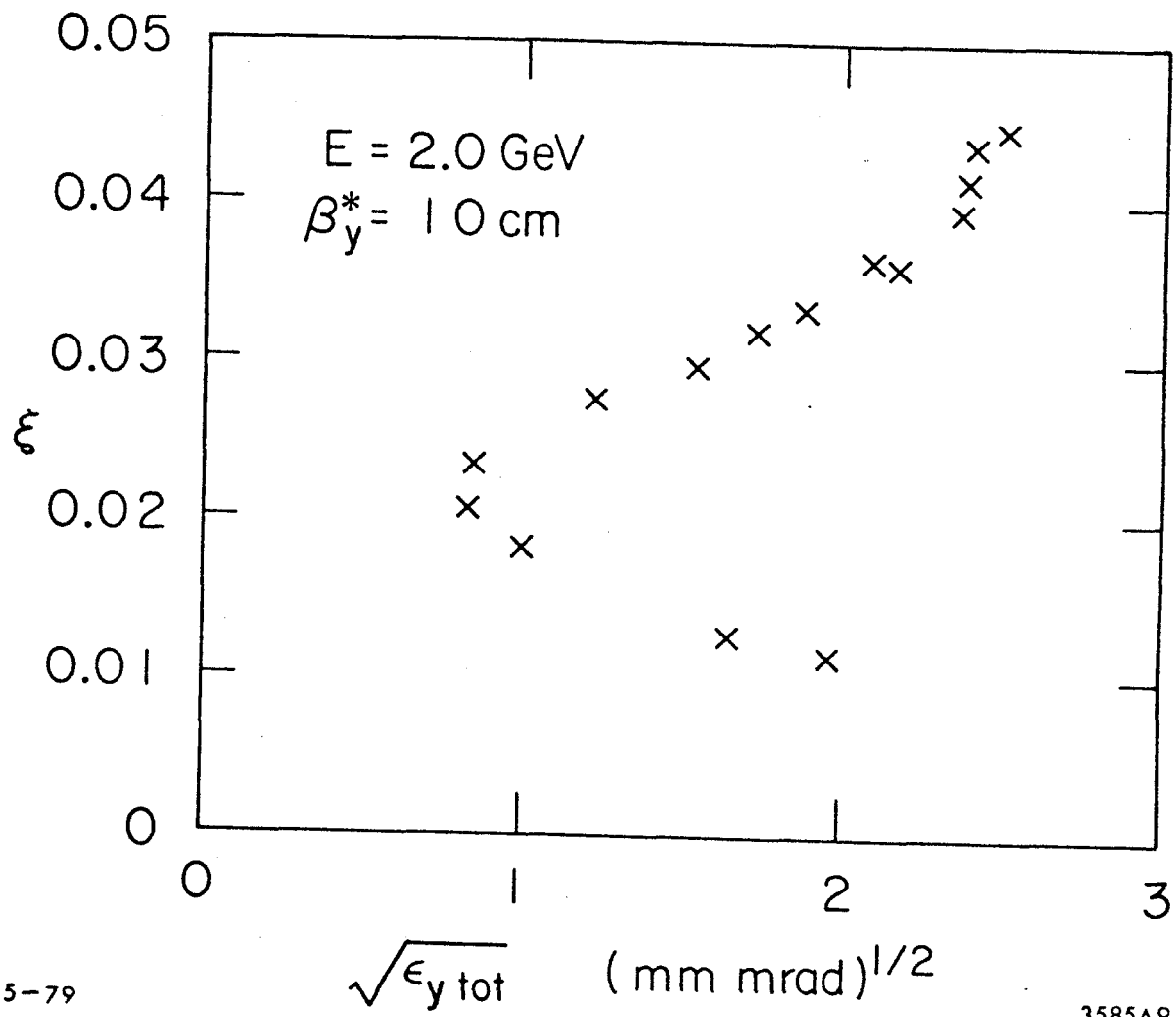


Fig. 9



5-79

3585A9

Fig. 10